A Framework for Evaluating the Resilience Contribution of Solar PV and Battery Storage on the Grid

Tyler Phillips
National & Homeland Security
Idaho National Laboratory
Idaho Falls, Idaho, USA
tylerphillips1@u.boisestate.edu

Timothy McJunkin
Power & Energy Systems
Idaho National Laboratory
Idaho Falls, Idaho, USA
timothy.mcjunkin@inl.gov

Craig Rieger
National & Homeland Security
Idaho National Laboratory
Idaho Falls, Idaho, USA
craig.rieger@inl.gov

John Gardner
Mechanical & Biomedical Engineering
Boise State University
Boise, Idaho, USA
jgardner@boisestate.edu

Hoda Mehrpouyan
Computer Science
Boise State University
Boise, Idaho, USA
hodamehrpouyan@boisestate.edu

***Abstract*—Motivated by decreased cost and climate change concerns, the penetration of solar photovoltaic (PV) energy generation and battery energy storage has been continually increasing. The variability in solar PV power generation has led to many new challenges for utilities and researchers. One challenge is the quantification of the resilience contribution to the grid from its assets and is the topic of this paper.**

In this work, we propose a framework for evaluating the resilience contribution of solar generation and battery storage assets on the grid. The metric provides a quantifiable adaptive capacity measure in terms of real and reactive power and includes uncertainty for solar PV assets. A case study using very short-term and short-term solar generation forecast demonstrates the framework and provides useful insight to the resilience solar and battery storage assets can contribute to the grid.

***Index Terms*—Resilience, Adaptive Capacity**

I. Introduction

The electrical power system is the most vital component of our nation's critical infrastructure. Modern society has become increasingly dependant on its ability to supply electrical power without interruption. Historically, reliability metrics have been adopted to ensure its continuous operation. However, there has been an increasing amount of distributed resource which provide intermitten and uncertain amounts of power generation. This has has presented utilities and researchers with new challenges.

Reliability metrics have not adequately prepared the electric grid for component failures during extreme events such as hurricanes, winter storms, flooding, and wildfires. In the U.S. between 2003 and 2012 extreme weather events caused an estimated 679 power outages that affected at least 50,000 customers [1]. Additionally, there has been an increasing frequency and intensity of these events due to climate change. A 2012 study [2] estimates the cost of weather related outages between $25 and $70 billion annually. Furthermore, prolonged power outages put the public safety at risk. Data indicates that the 2003 blackout in New York resulted in approximately 90 deaths [3]. In order to curb climate change, global action has been taken to reduce the amount of carbon emissions. In power generation, this has resulted in an increasing penetration of renewable sources like solar PV and wind power generation.

The increasing presence of renewable generation on the power system may have been spurred by climate change concerns. However, the dramatic reduction in investment have made it cost competitive with traditional resources. In early 2011, solar generation comprised less than 0.1% of the U.S. generation supply at just 3 gigawatts, by 2017 this number had grown to over 47 gigawatts. From 2010 to 2017, the adjusted cost for solar PV installed kilowatt-hour (kWh) dropped from $0.52 to $0.16 for residential, from $0.40 to $0.11 for commercial, and from $0.28 to $0.06 for utility scale generation. The Solar Energy Technologies Office set a 2030 goal for a further 50% reduction to $0.03 per kWh. Achieving this goal would make solar one of the cheapest sources of electricity generation and push further expansion of solar PV installation [4].

Integrating large amounts of variable and uncertain solar PV generation onto the electric grid is a growing concern. Power system operators accommodate for variability in system load and solar PV generation through systems of reserve power that can adjust output levels in dispatchable plants. In this context, the notional measure of resilience as defined by Woods [5] is how near a system is to its boundary, i.e. how much reserve power does the system have available.

This paper was supported by the U.S. Department of Energy's Office of Energy Efficiency and Renewable Energy under the Solar Energy Technology Office Award Number DE-0008775.

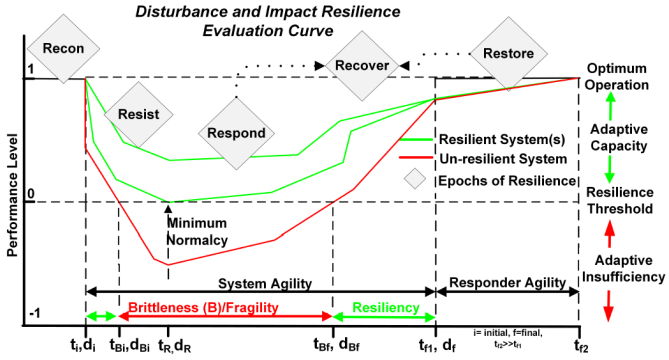

Fig. 1. The disturbance and impact resilience evaluation curve, showing the 5R's of resilience. Image adapted from [15].

Thus, resilience is a measure of the adaptive capacity of the system. In power systems, McJunkin and Rieger [6] introduced a resilience metric methodology based on assets aggregated adaptive capacity, in terms of real and reactive power, to quantify the system resilience looking forward in time. The metric was later extended to an operational metric in [7] with the ability to capture asymmetric assets, such as solar generation. The adaptive capacity of real and reactive power is of interest because it is used to maintain stability in both frequency and voltage. To maintain frequency, the balance of real power generation needs to meet demand, and the balancing of reactive power is needed to maintain voltage.

In this work, we present a metric based on the adaptive capacity to evaluate the resilience contribution that solar PV generation and battery storage add to the grid. The novelty of this paper is capturing the uncertainty of solar PV assets and its effect on the contribution it provides to the adaptive capacity of the grid. The reset of the paper is organized as follows; Section II introduces resilience applied to the power grid, as well as solar generation and its uncertainty. Section III provides the details of our resilience metric framework. We then carry out a case study in Section IV and give concluding remarks and future work in Section V.

II. Resilience in Power Systems

Hollnagel, Woods, and Leveson [8] introduced the resilience concept in engineering systems. Today, many definitions exist from well respected organizations [9]–[12], policy directives [13], and the academic community [14]. They all share a general commonality, resilience is the ability to anticipate a possible disaster, adopt effective measures to reduce losses or failures, and restore quickly. This is captured by the five "R's" of resilience; recon, resist, respond, recover, and restore, by the Disturbance and Impact Resilience Evaluation (DIRE) curve, shown in Fig. 1.

It can be seen that resilience is neither a short-term or long-term property. It encompasses time frames prior to the impact of the disturbance through the return to normalcy. The *recon*naissance phase requires the system to understand the state and forecast potential threats. System operators may focus on optimal economic efficiency rather than considering the response to an unexpected disturbance. However, some disturbances can be forecast and operators may consider valuing resilience of the system as well as economic efficiency. *Resist* is the phase which tends to be a measure of the inertial components of the system, such as spinning synchronous machines of generators and large motors. In general, the resist phase is of short duration. Assets which contribute to the resist phase slow the disturbance as opposed to devices that require measurements and control decisions in the *respond* phase through a control feedback loop. The respond phase consist of assets which provide real and reactive power as well as reconfiguration of the network to bring as much power back online to customers. *Restore* requires line crews to fix physical damage to the system and bring it to the pre disturbance level.

Rieger [15] presented the idea of the resilience threshold, or maximum acceptable level of degradation of the system. There are numerous metrics that can be used to quantify resilience, such as demand not served [16] and maximum number of customers out of service [17]. These metrics do a relatively good job at describing power system resilience, however, they do not capture the contribution from individual assets. Additionally, they look back in time and quantify resilience as the result of an event. Therefore, they do not give an operational perspective on resilience.

A. Solar PV Generation

The output of solar PV generation is variable due to the sun changing position throughout the day and seasons. This regularly leads to a 10% change in generation over 15 minutes. However, meteorological phenomena such as moving cloud cover, contribute to uncertainty in the generation and can cause rapid changes in power output. The size of the PV system, cloud speed, cloud height, and others factors influence the rate of change in power generation output. There is a rich body of literature on forecasting solar irradiance and PV generation. They can be broadly classified into four approaches; statistical based on historical measured data [18], artificial intelligence or machine learning such as neural networks [19], physics based numerical weather prediction models or satellite images [20], [21], and hybrid models [22].

The practical use of solar forecasting can be characterized at different time horizons. From the perspective of power system operation, very short-term (seconds to minutes) and short-term (up to 48-72 hours) forecast are particularly useful for activities like real-time unit scheduling, storage control, automatic generation control, and electricity trading [23]. Medium-term forecast consider week long forecast and can be used for maintenance scheduling, and long-term forecast are months or years and useful for solar PV plant planning. In this study, we consider very short-term and short-term time horizons which correlate to the respond and recover of the "R's" of resilience.

There are various evaluation indices to apply to forecasting accuracy. The commonly used indices include mean bias error, mean absolute error, mean square error, and root mean square error. These are all statistical formulas to measures of the

difference between the predicted forecast and measured data. The purpose of this work is not to cover the accuracy of solar forecast generation, but demonstrate how the uncertainty correlates to resilience of solar PV assets. In the following section, we cover the details of the purposed resilience framework.

III. Framework

In this section, we introduce the mathematical background for the resilience metric proposed for solar and battery storage assets. The metric is based on assets adaptive capacity and the following steps are taken for their calculation: determine the potential real and reactive power contribution, the flexibility from the operating point, consider temporal constraints, and then calculate the adaptive capacity.

A. Adaptive Capacity Calculation with Uncertainty

We begin by defining the potential contribution in real and reactive power an asset has on the grid. The power output of an asset is constrained by the apparent power in the complex S-plane and the limiting power output in the positive and negative plane. The apparent power in the S-plane is given as

$$S(\theta) = \sqrt{P^2 + Q^2} \tag{1}$$

where P and Q are the nameplate capacity in real and reactive power, respectively. Here the nameplate capacity is dependent on the real power plane. In the positive plane it is the nameplate capacity when the asset is a source. In the negative plane it is the nameplate capacity as a sink, i.e. a battery at max charging. The real and reactive power components of the apparent power are given as

$$P(\theta) = S\cos(\theta) \tag{2}$$

and

$$Q(\theta) = S\sin(\theta) \tag{3}$$

respectively. The power contribution of assets are limited by the apparent power and the limit of real power, therefore, the contribution limit of the asset is given as

$$P(\theta) = \begin{cases} \min\left[P(\theta),\ P_{\max}\right], & 0 \le \theta \le \frac{\pi}{2} \\ \min\left[P(\theta),\ P_{\max}\right], & \frac{3\pi}{2} \le \theta < 2\pi \\ -\min\left[|P(\theta)|,\ |P_{\min}|\right], & \frac{\pi}{2} < \theta < \frac{3\pi}{2} \end{cases} \tag{4}$$

where $P_{\max}$ and $P_{\min}$ are the maximum output as a source in the positive plane and the maximum output as a sink in the negative plane, respectively.

In the context of solar assets, which only contribute to the grid as a power source, the real power in the negative plane is zero, $P_{\min}$= 0. Additionally, solar assets don't have a constant real power contribution due to changes in solar intensity. This results in an uncertainty, u, in the maximum real power generation. Therefore, the contribution of real power from solar assets is limited by

$$P(\theta)_{\text{Solar}} = \begin{cases} \min\left[P(\theta),\ P_{\max} \pm u\right], & 0 \le \theta \le \frac{\pi}{2} \\ \min\left[P(\theta),\ P_{\max} \pm u\right], & \frac{3\pi}{2} \le \theta < 2\pi \\ 0, & \frac{\pi}{2} < \theta < \frac{3\pi}{2} \end{cases} \tag{5}$$

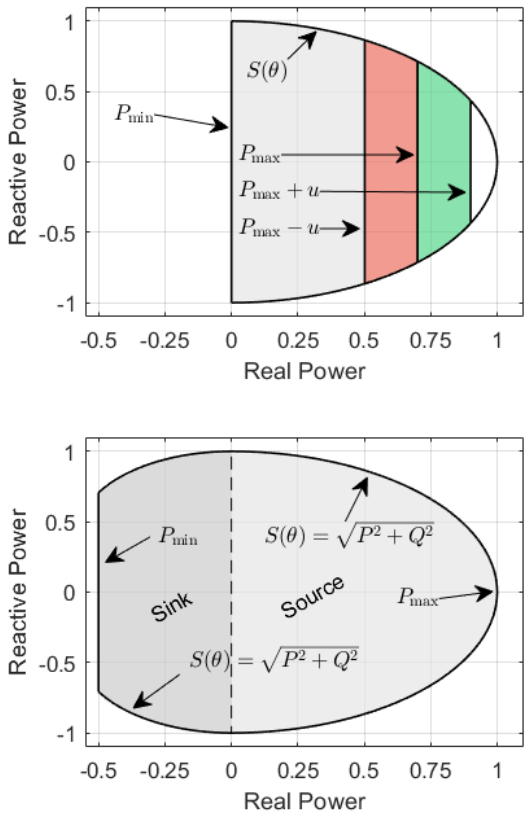

Fig. 2. Normalized power capability of a solar asset (top) and a battery asset (bottom). The positive uncertainty of the solar asset is shaded green and the negative in red.

The resulting output bounds of a solar asset is shown notionally by the normalized output in the top plot in Fig. 2. Here, the bounding constraints on the output $S(\theta)$, $P_{\min}$, and $P_{\max} \pm u$ can be seen. The green region represents the upper uncertainty, the red is the lower uncertainty, and the line between them is the maximum real power output, which is consider the forecasted output in this work.

On the other hand, battery storage assets may operate in both the positive and negative plane as a source and a sink. However, their nameplate capacity in real power in the positive and negative plane may not be the same. Therefore, the power in the negative plane in Equation 4 is not zero. The resulting contribution in real and reactive power of a battery storage asset is shown notionally by the normalized output in the bottom plot in Fig. 2. Here, it is shown that the battery asset can only operate at half the real power as a sink as when a source.

Next, we determine the flexibility of the asset which is a measure from the current operating point to the operating capability limits. Thus, the flexibility is a translation from P= 0, Q= 0 to the operating point P_0, Q_0. The limits of the operating power S, $P_{\max}$ and $P_{\min}$ take the form S', $P'_{\max}$, and $P'_{\min}$ after the translation for the flexibility. The flexibility

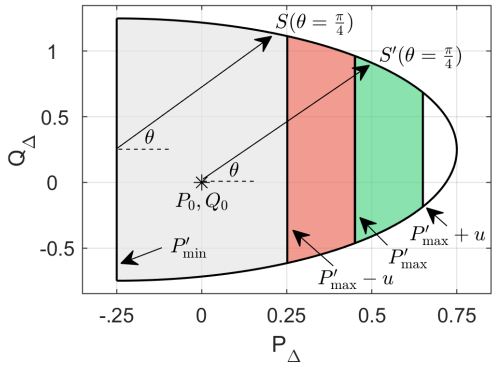

Fig. 3. Flexibility in real power (P_Δ) and reactive power (Q_Δ) of a normalized solar asset at current operation of P_0= 0.25 and Q_0= -0.25. The flexibility is a translation from $P = 0, Q = 0$ to the operation point.

in real power is given mathematically as

$$P_\Delta(\theta) = \begin{cases} \min\left[S'\cos(\theta),\ P'_{\max} \pm u\right], & 0 \le \theta \le \frac{\pi}{2} \\ \min\left[S'\cos(\theta),\ P'_{\max} \pm u\right], & \frac{3\pi}{2} \le \theta \le 2\pi \\ -\min\left[|S'\cos(\theta)|,\ |P'_{\min}|\right], & \frac{\pi}{2} < \theta < \frac{3\pi}{2} \end{cases} \quad (6)$$

here, battery assets have an uncertainty of zero. The flexibility in reactive power for both types of assets is given as

$$Q_\Delta(\theta) = S'\sin(\theta) \quad (7)$$

The flexibility of a solar asset with uncertainty is shown in Fig. 3, the current operation point is P = 0.25 and Q = -0.25.

Next, we consider the temporal limitations of the asset over the flexibility region. Temporal constraints include latency, ramp rates, and energy limitations. The latency, λ, is the time before a control action can make changes to the power output of the system. The ramp rate is how quick the asset can adjust the power output from the current operating point after the latency. The temporal constraint in real power is given as

$$P(t) = \begin{cases} 0, & t \le \lambda \\ \frac{dP}{dt}(t-\lambda), & t > \lambda \end{cases} \quad (8)$$

and the reactive power is

$$Q(t) = \begin{cases} 0, & t \le \lambda \\ \frac{dQ}{dt}(t-\lambda), & t > \lambda \end{cases} \quad (9)$$

where t is the future time from current operation. Ramp rates may be dependent on direction and non-linear, i.e. the asset may ramp down quicker than it can ramp up. We denote the the temporal real power ramping up as $P(t)^+$ and as $P(t)^-$ when ramping down. The same is done for the reactive power.

With the flexibility and temporal constraints, we can calculate the adaptive capacity at all power factor angles. The adaptive capacity in real power is given as

$$P_{\text{AC}}(\theta, t) = \begin{cases} \min\left[P_\Delta,\ P(t)^+\right], & 0 \le \theta \le \frac{\pi}{2} \\ \min\left[P_\Delta,\ P(t)^+\right], & \frac{3\pi}{2} \le \theta \le 2\pi \\ -\min\left[|P_\Delta|,\ |P(t)^-|\right], & \frac{\pi}{2} < \theta < \frac{3\pi}{2} \end{cases} \quad (10)$$

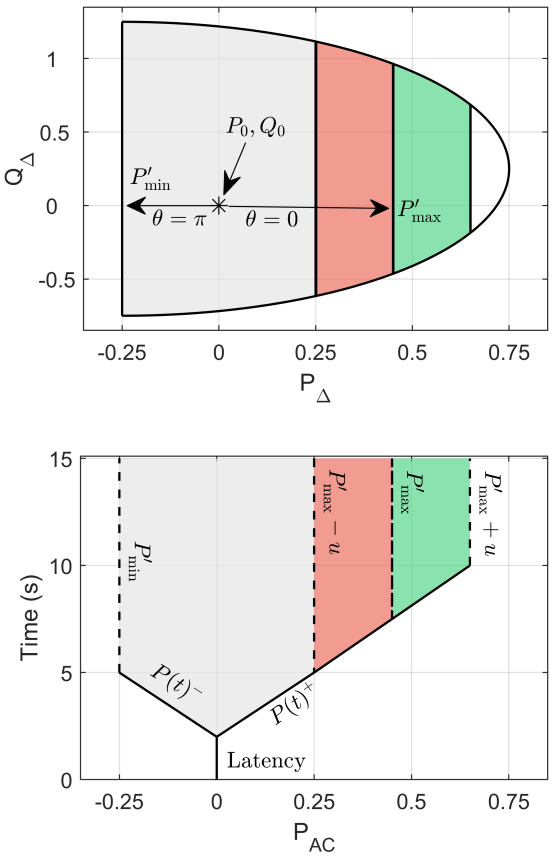

Fig. 4. Top plot shows the flexibility of a normalized solar asset and indicates the flexibility in real power at power factor angles of 0 and π. Bottom plot shows the real power flexibility from the operation point with latency and ramp rate constraints.

and the adaptive capacity in reactive power is given as

$$Q_{\text{AC}}(\theta, t) = \begin{cases} \min\left[Q_\Delta,\ Q(t)^+\right], & 0 \le \theta \le \pi \\ -\min\left[|Q_\Delta|,\ |Q(t)^-|\right], & \pi < \theta < 2\pi \end{cases} \quad (11)$$

The adaptive capacity in real power at a power factor angle of 0 and π is depicted in Fig. 4. In the top plot, it can be seen that the flexibility of the asset is constrained by the maximum and minimum power at these power factor angles. The bottom plot indicates the temporal constraints of the asset. The manifold shows the three dimensional view of these calculations at all power factor angles.

The adaptive capacity of assets can be aggregated together to give the adaptive capacity of a group of asset. The aggregation of real power is given as

$$P_{\text{AC}}(\theta, t) = \sum_{k=1}^{n} P_{\text{AC}_k} \quad (12)$$

and the reactive power is given as

$$Q_{\text{AC}}(\theta, t) = \sum_{k=1}^{n} Q_{\text{AC}_k} \quad (13)$$

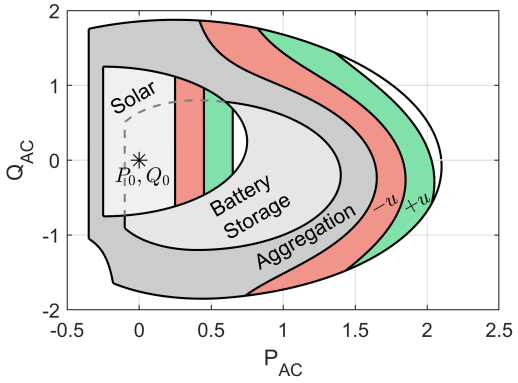

Fig. 5. Normalized adaptive capacity of solar and battery storage asset with operating point indicated by the data marker. Aggregation is shown and indicates the adaptive capacity of the system assets with uncertainty. Note, that temporal constraints are not considered here.

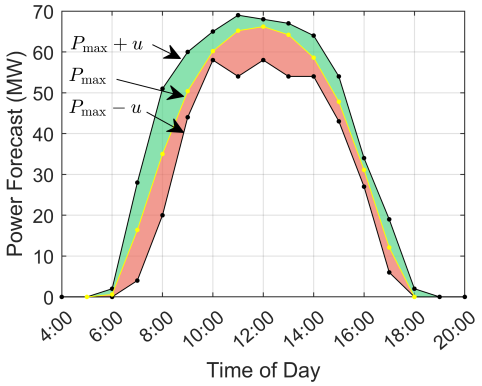

Fig. 6. Day-ahead solar forecast data. Yellow line represents the forecast ($P_{\max}$) and the green and red regions are the upper and lower uncertainty, respectively.

where n is the number of assets. The aggregation of a solar and battery asset is shown in Fig. 5. It can be seen that the aggregated adaptive capacity is the sum of the individual assets at any given power factor angle.

IV. Case Studies

In this section we demonstrate the resilience metric purposed in a case study using very short-term and short-term solar PV forecast data. First, we introduce the data set used in this study.

A. Solar Generation and Forecast Data Set

National Renewable Energy Laboratory (NREL) provides synthetic year long data for approximately 6,000 simulated PV plants[1]. The forecast data consist of 60-minute intervals for both day-ahead and 4 hour-ahead predictions. The data was generated using the 3TIER based on numerical weather predication simulations. In this work, solar data from Saturday, August 19th, 2006, in Arizona at location 33.45, -112.95 (latitude, longitude) was selected. The forecast data does not provide uncertainty, therefore, we generate uncertainty similar to that in [24]. We point out that the accuracy of uncertainty is not the focus of this work, but the effect it has on the adaptive capacity of solar PV generation. The forecast data and uncertainty used in the case studies is shown in Fig. 6. We begin with the very short-term forecast.

B. Very Short-term Power Forecast

Very short-term solar generation forecast are on the order of seconds or minutes. At this time scale the latency and ramp rate constraints are highly important for the assets adaptive capacity. To demonstrate the very short-term adaptive capacity of a solar PV asset we use the forecast data in Fig. 6 at noon. We apply a current power generation output of 50 MW, use a 1 second latency, and assume ramp rates for the real power in the positive and negative direction to be 10 MW/s and the reactive in both directions is 10 MVAR/s. The resulting adaptive capacity of the asset using the forecasted power data is shown by the yellow plot in the top plot of Fig. 7. In this figure, the red middle plot represents the negative uncertainty, and the green bottom plot represents the positive uncertainty. The plots have been zoomed in near the operating point to show the difference in the adaptive capacity in the positive real direction (all plots in the negative real direction are identical). It can be seen that when when solar generation is in the negative uncertainty direction the adaptive capacity in real power is very small. On the other hand, when it is in the positive uncertainty direction there is additional adaptive capacity in real power. In the following section, we will look at the short-term forecast using day-long forecast data.

[1]https://www.nrel.gov/grid/solar-power-data.html

C. Short-term Power Forecast

In this scenario, we consider the short-term power forecast to be day-ahead forecast power generation over a day, i.e. the full data shown in Fig. 6. We assume that the forecasted generation will be the operating point of the asset over the day. The results of the adaptive capacity, again near the origin to highlight the real power adaptive capacity differences, are shown in Fig. 8. Here, the top plot represents the asset adaptive capacity at the solar forecast, the middle represents the adaptive capacity for the negative uncertainty, and the lower plot represent the adaptive capacity for the positive uncertainty. It can be seen that when the forecast generation is correct the adaptive capacity in the positive real power direction is zero. When the generation is at the positive uncertainty the solar PV asset contributes to additional real power adaptive capacity, therefore adding to the resilience of the overall grid. On the other hand, when the generation is at the negative uncertainty the real power adaptive capacity is negative and the asset may be considered a disturbance on the power system. In this case, reserve power must be used in order to maintain the desired frequency of the grid. For this reason, we next consider the addition of battery storage to this scenario.

The additional battery storage asset is assumed to have a maximum power output of 20 MW as a source and -10 MW as a sink with ± 20 MVAR reactive capability. The operating

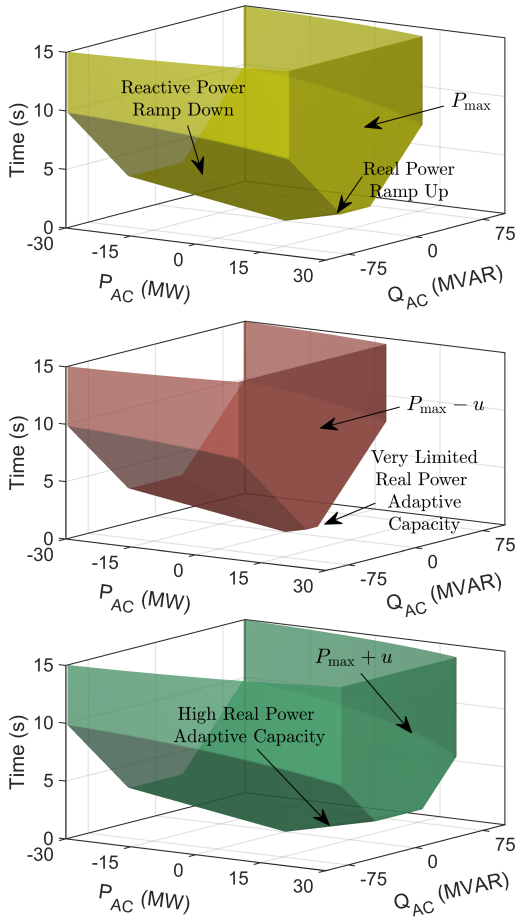

Fig. 7. Very short-term adaptive capacity at 12:00 noon assuming power output of 50 MW. Top plot represents forecast data, middle represents negative uncertainty, and the bottom is positive uncertainty.

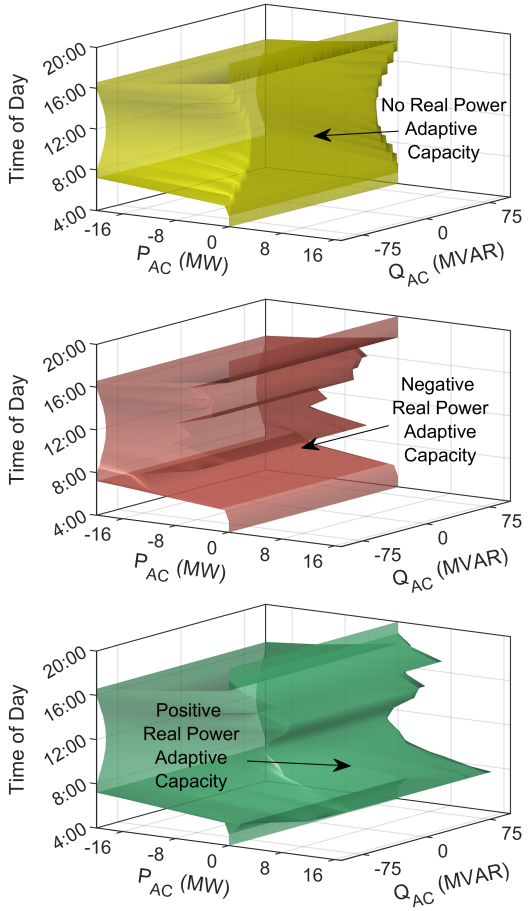

Fig. 8. Day-long adaptive capacity of the solar asset at forecast generation (top), negative uncertainty (middle), and positive uncertainty (bottom). Here the operation point is assumed to be the forecast output in each plot.

point is assumed to be idle, where $P_0 = 0$ and $Q_0 = 0$. The results of the aggregation of the solar adaptive capacity at negative uncertainty and the battery storage asset is shown in Fig. 9. It can be seen that the addition of the battery asset contributes to the adaptive capacity in the positive real power. Therefore, the system has the capability to respond to a disturbances in this direction, i.e. there is reserve power for an operator to maintain frequency stability of the system.

V. Conclusion and Future Work

This paper has provided a framework for considering the resilience contribution of solar and battery storage assets to the grid. The novel contribution is addition of uncertainty in adaptive capacity for solar generation assets. We demonstrated the metric in a case study using very sort-term (seconds) and short-term (day-long) solar forecast with uncertainty and provided the resilience that both the solar and battery assets contribute to the grid. It was demonstrated that when solar generation is above the forecast it provides additional adaptive capacity in the positive direction of real power. However, when it is below the forecasted generation, the adaptive capacity in the positive real power direction is negative, and may be considered a disturbance to the system. The addition of battery storage in this case demonstrated the ability to aggregate assets and provide the needed adaptive capacity in real power.

Future work includes implementation of the metric in a simulated environment such as Simulink or OPAL-RT. It is envisioned that the resilience metric will be used to influence the control decisions and result in a lower loss of power served to consumers during physical degradation and cyber attack scenarios.

Acknowledgment

This material is based upon work supported by the US Department of Energy's Office of Energy Efficiency and Renewable Energy (EERE) under the Solar Energy Technology Office Award Number DE-0008775. We thank our colleagues Professor Masood Parvania, Phd and Mohamad El Hariri, PhD. from the University of Utah who provided insight and expertise that assisted this research. Effort performed through Department of Energy under U.S. DOE Idaho Operations Office Contract DE-AC07-05ID14517, as part of the Resilient Control and Instrumentation Systems (ReCIS) program of Idaho National Laboratory.

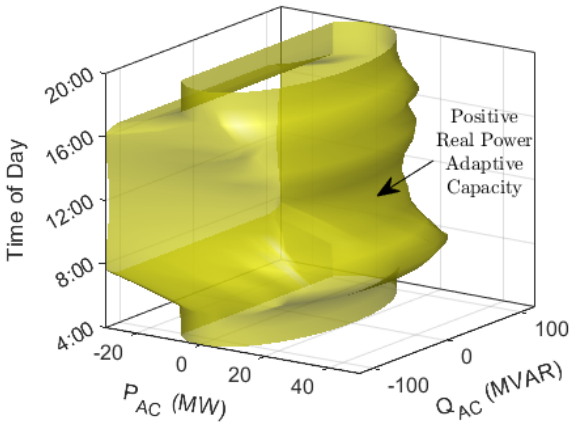

Fig. 9. Aggregation of day-long adaptive capacity of a solar asset at negative uncertainty (middle plot in Fig. 8) and battery storage asset at idle.

REFERENCES

[1] U.S. Department of Energy Office of Electricity Delivery and Energy Reliability, "Economic benefits of increasing electric grid resilience to weather outages," Executive Office of the President, Tech. Rep., 2013.

[2] R. Campbell, "Weather-related power outages and electric system resiliency," CRS Report for Congress, Tech. Rep., 01 2013.

[3] B. Anderson and M. Bell, "Lights out impact of the august 2003 power outage on mortality in new york, ny," *Epidemiology (Cambridge, Mass.)*, vol. 23, pp. 189–93, 03 2012.

[4] C. Murphy, Y. Sun, W. J. Cole, G. J. Maclaurin, M. S. Mehos, and C. S. Turchi, "The potential role of concentrating solar power within the context of doe's 2030 solar cost targets," 1 2019.

[5] D. Woods, *Resilience Engineering: Concepts and Precepts*. CRC Press, 2017.

[6] T. R. McJunkin and C. G. Rieger, "Electricity distribution system resilient control system metrics," in *2017 Resilience Week (RWS)*, Sep. 2017, pp. 103–112.

[7] T. Phillips, T. McJunkin, C. Rieger, J. Gardner, and H. Mehrpouyan, "An operational resilience metric for modern power distribution systems," in *2020 IEEE International Conference on Software Quality, Reliability and Security Companion (QRS-C), Requirements*, 2020.

[8] E. Hollnagel, D. Woods, and N. Leveson, *Resilience Engineering: Concepts and precepts*. Ashgate Publishing, 2006.

[9] National Acedemies of Sciences, Engineering, and Medicine, "Enhancing the resilience of the nation's electricity system," https://doi.org/10.17226/24836, 2017.

[10] Sandia National Laboratories, "Energy: Grid resilience," https://energy.sandia.gov/programs/electric-grid/resilient-electric-infrastructures/, accessed: 2/6/2020.

[11] H. Mehrpouyan, B. Haley, A. Dong, I. Y. Tumer, and C. Hoyle, "Resiliency analysis for complex engineered system design," *AI EDAM*, vol. 29, no. 1, pp. 93–108, 2015.

[12] H. Mehrpouyan, D. Giannakopoulou, G. Brat, I. Y. Tumer, and C. Hoyle, "Complex engineered systems design verification based on assume-guarantee reasoning," *Systems Engineering*, vol. 19, no. 6, pp. 461–476, 2016.

[13] U.S. Department of Homeland Security, "Presidential policy directive 21 implementation: An interagency security committee white paper," 2015.

[14] C. G. Rieger, D. I. Gertman, and M. A. McQueen, "Resilient control systems: Next generation design research," in *2009 2nd Conference on Human System Interactions*, May 2009, pp. 632–636.

[15] C. G. Rieger, "Resilient control systems practical metrics basis for defining mission impact," in *2014 7th International Symposium on Resilient Control Systems (ISRCS)*, Aug 2014, pp. 1–10.

[16] B. Johnson, V. Chalishazar, E. Cotilla-Sanchez, and T. K. Brekken, "A monte carlo methodology for earthquake impact analysis on the electrical grid," *Electric Power Systems Research*, vol. 184, p. 106332, 2020. [Online]. Available: http://www.sciencedirect.com/science/article/pii/S0378779620301383

[17] M. Kazama and T. Noda, "Damage statistics: Summary of the 2011 off the pacific coast of tohoku earthquake damage," *Soils and Foundation*, 2012.

[18] P. Bacher, H. Madsen, and H. A. Nielsen, "Online short-term solar power forecasting," *Solar Energy*, vol. 83, no. 10, pp. 1772 – 1783, 2009. [Online]. Available: http://www.sciencedirect.com/science/article/pii/S0038092X09001364

[19] A. Sfetsos and A. Coonick, "Univariate and multivariate forecasting of hourly solar radiation with artificial intelligence techniques," *Solar Energy*, vol. 68, no. 2, pp. 169 – 178, 2000. [Online]. Available: http://www.sciencedirect.com/science/article/pii/S0038092X9900064X

[20] R. Perez, E. Lorenz, S. Pelland, M. Beauharnois, G. Van Knowe, K. Hemker, D. Heinemann, J. Remund, S. C. Müller, W. Traunmüller, G. Steinmauer, D. Pozo, J. A. Ruiz-Arias, V. Lara-Fanego, L. Ramirez-Santigosa, M. Gaston-Romero, and L. M. Pomares, "Comparison of numerical weather prediction solar irradiance forecasts in the us, canada and europe," *Solar Energy*, vol. 94, pp. 305 – 326, 2013. [Online]. Available: http://www.sciencedirect.com/science/article/pii/S0038092X13001886

[21] E. Geraldi, F. Romano, and E. Ricciardelli, "An advanced model for the estimation of the surface solar irradiance under all atmospheric conditions using msg/seviri data," *IEEE Transactions on Geoscience and Remote Sensing*, vol. 50, no. 8, pp. 2934–2953, 2012.

[22] S. I. Nanou, A. G. Papakonstantinou, and S. A. Papathanassiou, "A generic model of two-stage grid-connected PV systems with primary frequency response and inertia emulation," *Electric Power Systems Research*, vol. 127, pp. 186 – 196, 2015. [Online]. Available: http://www.sciencedirect.com/science/article/pii/S0378779615001868

[23] C. Wan, J. Zhao, Y. Song, Z. Xu, J. Lin, and Z. Hu, "Photovoltaic and solar power forecasting for smart grid energy management," *CSEE Journal of Power and Energy Systems*, vol. 1, no. 4, pp. 38–46, 2015.

[24] S. F. Rafique, Z. Jian-hua, R. Rafique, J. Guo, and I. Jamil, "Renewable generation (wind/solar) and load modeling through modified fuzzy prediction interval," *International Journal of Photoenergy*, vol. 2018, pp. 1–14, 2018.